^{68}Ga-PSMA-11 PET/CT Improves Tumor Detection and Impacts Management in Patients with Hepatocellular Carcinoma

Nader Hirmas[1], Catherine Leyh[2], Miriam Sraieb[1], Francesco Barbato[1], Benedikt M. Schaarschmidt[3], Lale Umutlu[3], Michael Nader[1], Heiner Wedemeyer[2], Justin Ferdinandus[1], Christoph Rischpler[1], Ken Herrmann[1], Pedro Fragoso Costa[1], Christian M. Lange[2], Manuel Weber[*1], and Wolfgang P. Fendler[*1]

[1]*Department of Nuclear Medicine, University of Duisburg–Essen and German Cancer Consortium–University Hospital Essen, Essen, Germany;* [2]*Department of Gastroenterology and Hepatology, University Hospital Essen, University of Duisburg–Essen, Essen, Germany; and* [3]*Institute of Diagnostic and Interventional Radiology and Neuroradiology; University Hospital Essen, University of Duisburg–Essen, Essen, Germany*

Hepatocellular carcinoma (HCC) is the sixth most prevalent cancer and the third most frequent cause of cancer-related death. A growing number of local and systemic therapies are available, and accurate staging is critical for management decisions. We assessed the impact of neovasculature imaging by ^{68}Ga-PSMA-11 PET/CT on disease staging, prognostic groups, and management of patients with HCC compared with staging with CT. **Methods:** Forty patients who received imaging with ^{68}Ga-PSMA-11 PET/CT for HCC staging between September 2018 and September 2019 were retrospectively included. Management before and after PET scanning was assessed by standardized surveys. The presence of HCC was evaluated by 3 masked readers on a per-patient and per-region basis for PET/CT (PET criteria) and multiphase contrast-enhanced CT (CT criteria) in separate sessions. Lesions were validated by follow-up imaging or histopathology, and progression-free survival was recorded. Endpoints were detection rate and positive predictive value for ^{68}Ga-PSMA-11 PET versus CT, interreader reproducibility, and changes in stage, prognostic groups, and management plans. **Results:** Median age was 65 y (range, 37–81 y), and median Child–Pugh score was 5 (range, 5–9). Most patients were treatment-naïve (27/40, 67.5%). The sensitivity of PET versus CT to identify liver lesions for patients with lesion validation was 31 of 32 (97%) for both modalities, whereas it was 6 of 6 (100%) versus 4 of 6 (67%), respectively, for extrahepatic lesions. PET and CT each had a positive predictive value of 100% at the liver level. PET versus CT stage was congruent in 30 of 40 (75%) patients; upstaging was seen in 8 of 40 patients (20%), whereas 2 of 40 (5%) had downstaging by PET. Intended management changed in 19 of 40 patients (47.5%); 9 of 19 of these patients were found to have detectable distant metastases (47.4%) and assigned stage 4 disease, most of whom were shifted to systemic therapy (8/9, 89%). Two patients underwent ^{177}Lu-PSMA-617 radioligand therapy. Median progression-free survival was 5.2 mo for the entire cohort; 5.3 mo for PET M0, and 4.7 mo for PET M1 patients, respectively. **Conclusion:** ^{68}Ga-PSMA-11 PET demonstrated higher accuracy than CT in the detection of HCC metastases and was associated with a management change in about half the patient cohort.

Key Words: hepatocellular carcinoma; PSMA; PET; staging; theranostic

J Nucl Med 2021; 62:1235–1241
DOI: 10.2967/jnumed.120.257915

Hepatocellular carcinoma (HCC) is the sixth most prevalent cancer and the third most frequent cause of cancer-related death worldwide (*1*).

Early-stage HCC is often treated with surgical resection, transplantation, or ablation, whereas systemic therapy, transarterial chemoembolization (TACE), and radioembolization (also known as selective internal radiation therapy [SIRT]) are reserved for intermediate to advanced HCC, with SIRT being most often used after progression under sorafenib (*2,3*). The treatment landscape for HCC changed considerably with the availability of life-prolonging systemic therapy. Despite recent therapy approvals, patient survival remains short, and accurate staging is critically needed for early identification of candidates for the various local and systemic therapies. The European Society for Medical Oncology guidelines recommend CT, MRI, or ultrasound for diagnosis of HCC in patients with cirrhosis (*4*). However, small HCC lesions may be hard to detect, especially with concomitant cirrhosis.

^{68}Ga-PSMA-11 is a novel PET tracer that has been developed for imaging patients with prostate cancer (*5,6*). Prostate-specific membrane antigen (PSMA) was also found to be expressed on the neovasculature of other tumor entities (*7,8*), with immunohistochemistry revealing PSMA expression on HCC neovasculature and canalicular membranes, with significantly increased uptake in hepatic and extrahepatic disease (*9,10*). A recent prospective study on 15 patients with HCC reported improved lesion detection with ^{68}Ga-PSMA-11 PET/CT compared with conventional imaging and a subsequent impact on treatment strategies (*11*).

In light of increasing local and systemic treatment options, ^{68}Ga-PSMA-11 PET/CT may demonstrate value for staging and management of patients with initial HCC. In this study, we aimed to assess the accuracy of ^{68}Ga-PSMA-11 PET/CT along with interreader agreement and impact on staging, management, and prognostic groups in patients with initial HCC.

Received Oct. 2, 2020; revision accepted Dec. 28, 2020.
For correspondence or reprints, contact Wolfgang P. Fendler (wolfgang.fendler@uk-essen.de).
*Contributed equally to this work.
Published online January 28, 2021.

MATERIALS AND METHODS

Study Design and Participants

Patients undergoing ^{68}Ga-PSMA-11 PET/CT for HCC between September 2018 and September 2019 at the Essen University Hospital were retrospectively included in the study. The primary endpoint was detection rate and positive predictive value for ^{68}Ga-PSMA-11 PET versus CT. Secondary endpoints were interreader reproducibility and changes in stage, prognostic group, and management plans. All patients gave written consent to undergo clinical ^{68}Ga-PSMA-11 PET/CT. The retrospective study was approved by the ethics committee at the University Duisburg–Essen (approval 19-8892-BO), and the need for study-specific consent was waived. Anonymized study data were collected retrospectively and managed using the Research Electronic Data Capture (REDCap) electronic data capture tools hosted at the University Hospital Essen (*12,13*). Patients' records were accessed to retrieve demographic and clinical data, pathology and lab investigations, and imaging studies performed before or after ^{68}Ga-PSMA-11 PET/CT.

Imaging Procedures

^{68}Ga-PSMA-11 (Glu-NH-CO-NH-Lys-(Ahx)-[^{68}Ga(HBED-CC)]) was labeled in accordance with the joint procedure guideline of the European Association of Nuclear Medicine and the Society of Nuclear Medicine and Molecular Imaging (*14*). PET was performed in accordance with the international guidelines as part of a PET/CT scan and with a field of view from the skull base to the mid thigh. Patients received a median of 112.5 MBq (range, 79–344 MBq) of ^{68}Ga-PSMA-11. Image acquisition was started at a median of 78 min after injection (range, 50–135 min; with an interquartile range of 31.5).

All 40 examinations were performed with radiographic contrast enhancement in the arterial and portal venous phases; contrast-enhanced CT was performed before the PET acquisition. Images were acquired using a Siemens Biograph 128 mCT device in 29 of 40 cases (72.5%) and a Siemens Biograph Vision in 11 of 40 cases (27.5%); both devices are cross-calibrated based on EANM Research Ltd. accreditation standards. PET images were reconstructed by ordered-subset expectation maximization–based algorithms. Data from CT scans were used for attenuation correction and anatomic correlation.

Image Interpretation

Three nuclear medicine physicians masked to all clinical and imaging data interpreted the images separately—first, the attenuation-corrected ^{68}Ga-PSMA-11 PET and CT images using PET criteria, and 2 wk later, CT images only using CT criteria. OsiriX MD (Pixmeo SARL) was used for the readings.

The presence of HCC lesions was recorded separately for ^{68}Ga-PSMA-11 PET and CT across 5 regions (positive/negative): liver segments, abdominal and extraabdominal lymph nodes, peritoneal/visceral lesions, and bone lesions.

For PET interpretation only, a 4-point scale was used to visually rate focal radioligand uptake (from 0 to 3) (*15,16*), with the corresponding CT scans used for anatomic correlation. Focal uptake was considered positive if the score was at least 1 (extrahepatic lesions) or at least 2 (hepatic lesions). Differentiating between HCC lesions and dysplastic nodules on CT scans (or MRI scans in cases of follow-up imaging) followed the criteria outlined in Supplemental Table 1 (supplemental materials are available at http://jnm.snmjournals.org) (*17,18*).

Readers recorded the SUV_{max} for the lesions with the highest uptake and diameter of the largest lesions (short axis for lymph nodes, long axis for all other lesions) at a given region. Readers determined the TNM staging separately for ^{68}Ga-PSMA-11 PET and CT in accordance with the criteria of the American Joint Committee on Cancer, eighth edition (*19*).

Consensus (positive vs. negative) was determined by a statistic majority vote among the 3 readers, with average values taken for quantitative values (SUV_{max} and lesion size). Consensus findings for the ^{68}Ga-PSMA-11 PET and CT scans for each patient were compared to determine concordance.

Lesion Validation and Change in Management

Patient files were reviewed for correlative and follow-up information acquired during routine clinical follow-up. CT, MRI, bone scans, and ^{68}Ga-PSMA-11 PET scans performed as preimaging and on follow-up were included in this analysis.

The most valuable comparator, with the following priority order (highest to lowest), was used to assign true or false positivity and negativity to detected lesions: histopathology from biopsies or surgical excision took priority over imaging validation; lesions were also confirmed by presence on the initial and follow-up scans, as well as their change in size, disappearance, or appearance on follow-up imaging during treatment, using modified RECIST (*20*). Any lesion that could not be verified on the basis of those criteria was excluded from the accuracy analyses. The local investigators interpreted the composite reference standard after reviewing follow-up information.

The management plan before PET was local therapy, including SIRT, radiofrequency ablation, or TACE, as documented by the interdisciplinary tumor board. The implemented management after PET was recorded by the referring physician using a standardized survey.

Statistical Analysis

Descriptive statistics were calculated. Interobserver agreement was determined by the Fleiss κ and interpreted by the criteria of Landis and Koch (*21*). The positive predictive value, negative predictive value, sensitivity, and specificity of ^{68}Ga-PSMA-11 PET on a per-patient and per-region basis for detection of tumor location, as confirmed by histopathology or biopsy, clinical follow-up, and conventional imaging follow-up, were calculated via standard 2×2 tables. PET progression-free survival was calculated from the date of the ^{68}Ga-PSMA-11 PET scan until progression, death, or last follow-up. κ analysis was performed using R statistics (version 3.4.1).

RESULTS

Patient Characteristics

Forty patients were included; their characteristics are outlined in Table 1. The median age was 65 y (range, 37–81 y). Twenty patients (50%) had histopathologic confirmation of HCC; the other half had imaging findings consistent with HCC. Liver cirrhosis was present in 28 of 40 patients (70%). The most frequent underlying liver disease was chronic hepatitis B or C, in 18 of 40 patients (45%). In addition, portal vein thrombosis or invasion was seen in 9 of 40 patients (22.5%). Eleven patients (27.5%) had ascites. Twenty-seven patients (67.5%) did not receive treatment before their ^{68}Ga-PSMA-11 PET scan.

Detection Accuracy and Lesion Validation

In total, 142 lesions from 36 patients were validated as true-positive, false-positive, or false-negative at the levels of the hepatic segments (1 through 8) and extrahepatic metastases. Lesions from 8 patients (20%) were validated by histopathology, 26 of 40 (65%) by baseline and follow-up imaging correlation and 10 of 40 (25%) by baseline imaging correlation only. All patients with histopathologic verification had follow-up imaging performed.

^{68}Ga-PSMA-11 PET versus CT accuracy for the liver lobes and distant metastases is reported in Table 2. Consensus interpretation on a whole-liver level for the entire cohort and for patients with cirrhosis (28/40, 70%) resulted in an accuracy of 97% for both

TABLE 1
Patient Characteristics ($n = 40$)

Characteristic	Data
M:F ratio	5.7:1
Age at diagnosis (y)	65 (37–81)
Primary diagnostic investigations	
Histopathology	20 (50)
Imaging	31 (77.5)
α-fetoprotein level	19 (47.5)
Comorbidities	
Cirrhosis	28 (70)
Hepatitis B or C	18 (45)
Diabetes	11 (27.5)
Nonalcoholic steatohepatitis/steatosis	5 (12.5)
Portal vein thrombosis or invasion	9 (22.5)
Ascites	
None	29 (72.5)
Controlled	10 (25)
Refractory	1 (2.5)
Baseline investigations	
Body mass index (kg/m^2)	27.4 (20.2–38.5)
α-fetoprotein (ng/mL)	36.1 (1–19,078)
Total bilirubin (μmol/L)	0.8 (0.2–6.7)
Albumin (g/L)	4.1 (2.6–5)
International normalized ratio	1.1 (1–1.6)
Alkaline phosphatase (IU/L)	127 (33–937)
Child–Pugh score	5 (5–9)
Class A	33 (82.5)
Class B	7 (17.5)
Treatment received before PSMA PET/CT	
None	27 (67.5)
Systemic treatment	2 (5)
Surgery	6 (15)
TACE or radiofrequency ablation	14 (35)
SIRT	4 (10)

Qualitative data are number and percentage; continuous data are median and range.

^{68}Ga-PSMA-11 PET and CT (sensitivity of 97%, specificity and positive predictive value of 100%, and negative predictive value of 80%). Liver segment–level data for detection rate and accuracy are given in Supplemental Table 2.

^{68}Ga-PSMA-11 PET versus CT detected 13 versus 9 distant metastatic lesions in 11 versus 8 patients, respectively (Table 3). Extrahepatic lesions were validated in 6 patients on further follow-up: sensitivity for ^{68}Ga-PSMA-11 PET versus CT was 100% versus 67%, respectively, and the negative predictive value was 100% versus 93%, respectively (Table 2).

Of the cases with congruence in ^{68}Ga-PSMA-11 PET and CT, 1 patient had disseminated bone metastases on preimaging that were confirmed on ^{68}Ga-PSMA-11 PET and CT (Supplemental Fig. 1); another patient had mediastinal lymph node metastases on ^{68}Ga-PSMA-11 PET and CT that were subsequently verified as positive by histopathology after lymph node resection (Supplemental Fig. 2); and a third patient had pathologic lymph nodes in the cardiophrenic angle that were confirmed on follow-up scans (Supplemental Fig. 3).

Among the cases in which ^{68}Ga-PSMA-11 PET outperformed CT, one patient had positive PSMA uptake in the right femur on ^{68}Ga-PSMA-11 PET that was missed on CT (Supplemental Fig. 4), and follow-up CT scans for that patient confirmed development of an osseous lesion. Another patient, with positive PSMA uptake in the right fourth rib seen on ^{68}Ga-PSMA-11 PET but not on CT (Supplemental Fig. 5), had subsequent scans confirming resolution of the lesion after local treatment to the metastatic spot. A third patient had metastatic lesions in mediastinal lymph nodes and lumbar vertebra that were not deemed pathologic on CT (Supplemental Figs. 6-I and 6-II) and was offered systemic treatment as a result. In the remaining patients with lesion validation, distant metastases were ruled out by both ^{68}Ga-PSMA-11 PET and CT and were subsequently confirmed as negative on follow-up imaging.

Interobserver Agreement

According to the Fleiss κ, agreement among the 3 independent readers for PET versus CT at the liver level was 0.43 (95% CIs, 0.25–0.61) versus 0.56 (95% CIs, 0.38–0.74), respectively, indicating moderate agreement according to the Landis and Koch criteria. At the extrahepatic level (lymph nodes and osseous metastases), agreement for PET versus CT was 0.83 (95% CIs, 0.65–1.01) versus 0.75 (95% CIs, 0.56–0.93), respectively. This corresponds to almost perfect agreement for PET and substantial agreement for CT, according to the same criteria.

Staging Concordance and Migration

Comparison of staging between ^{68}Ga-PSMA-11 PET and CT is shown in Tables 3 and 4. Concordance between ^{68}Ga-PSMA-11 PET and CT findings was seen in 30 of 40 patients (75%), whereas 8 of 40 patients (20%) experienced upstaging and 2 of 40 (5%) had downstaging by ^{68}Ga-PSMA-11 PET (Supplemental Table 3).

With regard to upstaged patients, 1 patient (2.5%) with no disease on CT was upstaged to post-PET stage 2. In this patient, a single lesion in liver segment 5 was found by ^{68}Ga-PSMA-11 PET and missed by CT, as confirmed by histopathology (Supplemental Fig. 7). In addition, 6 of 40 patients (15%) with CT stage 2 were upstaged to post-PET stage 3 ($n = 4$, 10%) and stage 4 ($n = 2$, 5%), and 1 patient (2.5%) with CT stage 3 was upstaged to post-PET stage 4.

In total, there were 3 of 40 patients (7.5%) in whom ^{68}Ga-PSMA-11 PET detected distant disease that was not detected by CT. The cases were detailed previously above and in Supplemental Figures 4, 5, and 7.

Downstaging by ^{68}Ga-PSMA-11 PET occurred in 2 patients: 1 had CT stage 2 (lesion diameter, 3.4 cm), but ^{68}Ga-PSMA-11 PET did not detect any hepatic disease. Follow-up MRI showed a lesion in segment V (diameter, 2.9 cm); hence, the ^{68}Ga-PSMA-11 PET result was deemed false-negative. The other patient had a CT stage 3B (T4N0M0) but a PET stage 3A (T3N0M0), with no implications on management in this case.

A summary of concordant and discordant staging between ^{68}Ga-PSMA-11 PET and CT is shown in Table 4. Mean lesion

TABLE 2
Accuracy, Sensitivity, Specificity, Positive Predictive Value, and Negative Predictive Value Between PSMA PET and CT

	Whole-liver analysis		Right lobe (segments 1 and 4–8)		Left lobe (segments 2 and 3)		Distant metastases	
Parameter	PSMA PET	CT	PSMA PET	CT	PSMA PET	CT	PSMA PET	CT
Accuracy (%)	97	97	97	94	86	91	100	94
Sensitivity (%)	97	97	97	94	77	85	100	67
Specificity (%)	100	100	100	100	91	95	100	100
Positive predictive value (%)	100	100	100	100	83	92	100	100
Negative predictive value (%)	80	80	83	67	87	91	100	93

size on CT and mean SUV_{max} on ^{68}Ga-PSMA-11 in different stages are summarized in Supplemental Table 4.

Management Follow-up

Figure 1 illustrates changes in management after ^{68}Ga-PSMA-11 PET for different stage groups. Overall, pre- to post-PET/CT treatment plans changed in 19 of 40 patients (47.5%).

^{68}Ga-PSMA-11 PET detected no correlate of disease in 4 of 40 patients (10%). Among these, 1 of 4 patient (25%) experienced a change in management, that is, a switch from SIRT to TACE. This change was based on the original unmasked imaging report, which had reported tumor foci in the liver; such findings were not reported in the consensus readings by the masked readers and were thus considered negative.

TABLE 3
Comparison of Staging Between PSMA PET and CT Scans

Stage	PSMA PET	CT
Stage 0 (T0N0M0)	4 (10)	4 (10)
Stage 2 (T2N0M0)	5 (12.5)	11 (27.5)
Stage 3	20 (50)	17 (42.5)
3A: T3N0M0	17 (42.5)	13 (32.5)
3B: T4N0M0	3 (7.5)	4 (10)
Stage 4B	11 (27.5)	8 (20)
T0N0M1 (bone)	1 (2.5)	—
T2N0M1	4 (10)	4 (10)
Bone	2 (5)	1 (2.5)
Mediastinal LN	1 (2.5)	2 (5)
Mediastinal LN + bone	1 (2.5)	1 (2.5)
T3N0M1	5 (12.5)	2 (5)
Bone	2 (5)	1 (2.5)
Mediastinal LN	1 (2.5)	—
Mediastinal LN + bone	1 (2.5)	—
Cardiophrenic recess	1 (2.5)	1 (2.5)
T4N0M1 (bone)	1 (2.5)	2 (5)

LN = lymph node.
Data are number followed by percentage in parentheses.

^{68}Ga-PSMA-11 PET detected stage 2 disease in 5 of 40 patients (12.5%). Among these, 2 of 5 patients (40%) experienced a change in management as follows: one was shifted from SIRT to systemic therapy, and the other was shifted to TACE from active surveillance.

Twenty patients (50%) were classified as stage 3 by ^{68}Ga-PSMA-11 PET, 7 of whom (35%) had a shift in management as follows: 6 were switched to systemic therapy because of evident portal vein or mesenteric vein thrombosis ($n = 3$), a proven high risk for a hepatopulmonary shunt ($n = 1$), or being deemed not suitable for SIRT treatment ($n = 2$); the remaining patient was switched to best supportive care.

Eleven patients (27.5%) were classified as stage 4 by ^{68}Ga-PSMA-11 PET. The highest rate of change in management occurred in patients with stage 4B, recorded in 9 of 11 (82%), 8 of whom (89%) were shifted to systemic therapy on detection of distant metastases on ^{68}Ga-PSMA-11 PET scan; TACE was performed in the remaining patient (Supplemental Fig. 5). Details of management changes before and after ^{68}Ga-PSMA-11 PET are highlighted in Supplemental Table 5.

Two patients had liver lesions with high uptake on ^{68}Ga-PSMA-11 PET; those patients had no other local or systemic treatment options, and they were deemed eligible for and proceeded with ^{177}Lu-PSMA-617 radioligand therapy. However, as revealed by intratherapeutic SPECT/CT-based dosimetry, the tumor radiation dose by radioligand therapy was at least 10-fold lower than typically achieved by 1 cycle of external-beam radiation therapy for HCC, and as such, this treatment modality was not as effective as anticipated. Radioligand therapy was discontinued after 1 cycle for both patients. Radioligand therapy and dosimetry findings are summarized in Supplemental Figures 8 and 9.

Progression-Free Survival Outcomes

The median observation period was 8.3 mo (range, 0.2 to 18.1 mo) from ^{68}Ga-PSMA-11 PET/CT. Patients with observation periods of less than 6 mo were either deceased ($n = 9/40$, 22.5%) or lost to follow-up ($n = 4/40$, 10%). During the observation period, disease progression after initial ^{68}Ga-PSMA-11 PET was noted for 26 of 40 patients (65%) as follows: 13 of 40 by follow-up imaging (32.5%) and 13 of 40 by death (32.5%). For the remaining patients, 4 of 40 (10%) were lost to follow-up, and 10 of 40 (25%) are still on regular follow-up at our institution.

Median progression-free survival was 5.2 mo. Patients with PET M0 versus M1 disease had a median progression-free survival of 5.3 mo versus 4.7, respectively ($P = 0.865$).

TABLE 4
Stage Migration Through PSMA PET and CT

	PSMA PET				
CT	No disease	Stage 2	Stage 3A	Stage 3B	Stage 4B
No disease	3 (7.5)	1 (2.5)*	0	0	0
Stage 2	1 (2.5)†	4 (10)	4 (10)*	0	2 (5)*
Stage 3A	0	0	12 (30)	0	1 (2.5)*
Stage 3B	0	0	1 (2.5)†	3 (7.5)	0
Stage 4B	0	0	0	0	8 (20)

*PET upstaging.
†PET downstaging.
Data are number followed by percentage in parentheses.

DISCUSSION

We compared ^{68}Ga-PSMA-11 PET and CT accuracy for HCC lesion detection and assessed the impact of PET on management and prognostic groups. Our results demonstrate comparable accuracy between ^{68}Ga-PSMA-11 PET and CT for staging at the liver level, with superior performance for ^{68}Ga-PSMA-11 PET at the extrahepatic level (almost perfect agreement among the independent readers). PET/CT accuracy was associated with a management change, particularly in patients with advanced disease, leading to a shift toward systemic therapy. PET detection of extrahepatic disease was not associated with shorter progression-free survival.

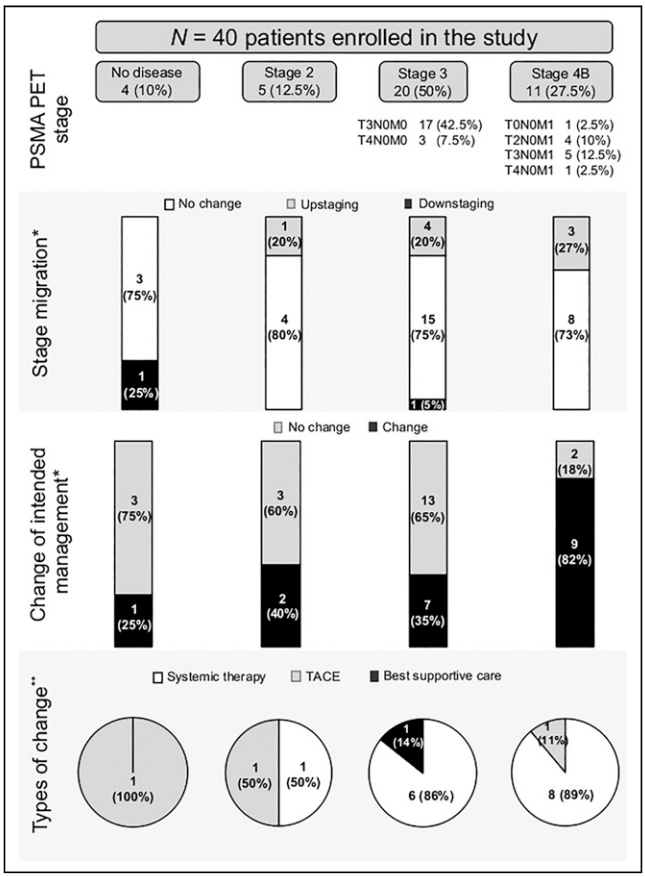

FIGURE 1. PSMA PET stage and change in management. *% from PSMA PET stage. **% from changed management.

HCC treatment decisions depend on a multidisciplinary approach that takes into account several factors, including size, extent of tumor burden, and functional status of the liver (*22*). For intermediate- and advanced-stage disease, the standard of care includes radiofrequency ablation, TACE, SIRT, or systemic therapy, whereas patients with end-stage disease often receive palliative care only (*2,23–25*). Most patients with HCC present with advanced disease and a poor prognosis (*26,27*). Imaging is critical to accurately assess local and distant disease extent at baseline and follow-up, thereby refining identification of candidates for systemic treatment.

Currently, international treatment guidelines place sorafenib as the standard first-line systemic therapy for patients with advanced HCC or earlier-stage tumors progressing on or unsuitable for locoregional therapies (*2,23–25*). Current Food and Drug Administration–approved first-line treatments for advanced or progressive HCC are sorafenib or lenvatinib, which are associated with prolonged survival in patients with advanced tumors (*28–30*). New options include bevacizumab in combination with atezolizumab as first-line therapy, as well as regorafenib, cabozantinib, and ramucirumab, in addition to immunotherapy agents such as nivolumab and pembrolizumab, as second-line therapies (*31*). PSMA-directed systemic treatments such as mipsagargin have also been recently studied, with preliminary results showing prolonged disease stabilization in patients with HCC who progressed on or after sorafenib or were intolerant to it (*32*).

^{68}Ga-PSMA-11 PET identified distant disease earlier and led to a change toward systemic treatment in our study. In this nonrandomized observational setting, progression-free survival was not significantly different for PET M0 versus M1 patients. PET may contribute to an improved outcome for metastatic HCC through earlier identification of candidates for systemic therapy. However, assessment in a prospective trial is needed, as our retrospective observation is limited to the assessment of stage migration with reported impact on management.

A systematic review and metaanalysis summarized the existing evidence on multiphasic CT versus MRI accuracy for the diagnosis of HCC in patients with underlying cirrhosis (*33*). A pooled analysis of the 19 studies comparing both modalities showed

significantly higher sensitivity (0.82 vs. 0.66) and a lower negative likelihood ratio (0.20 vs. 0.37) for MRI than for CT. In our study, ^{68}Ga-PSMA-11 PET and CT had a similar detection rate and accuracy at the liver level for both the entire cohort and the subset of patients with cirrhosis. Thus, PET will not replace MRI for accurate liver staging. Underlying cirrhosis did not affect lesion PSMA uptake (median SUV_{max} for patients with cirrhosis and for those without cirrhosis was 14.1).

HCC diagnosis is based more often on imaging than on biopsy (*2*); therefore, histopathologic information pertaining to tumor grade and aggressiveness is often missing. ^{18}F-labeled choline derivatives, such as ^{18}F-fluorethylcholine and ^{18}F-fluorocholine, have demonstrated value in identifying differentiated, less aggressive HCC, whereas ^{18}F-FDG is useful in identifying less differentiated, more aggressive tumor forms (*34*). In 1 study, dual-tracer PET/CT (using ^{18}F-fluorocholine and ^{18}F-FDG) enabled stage upgrading in 11% of patients and treatment modification in 14% (*35*). With documented expression of PSMA in tumor neovasculature and canalicular membranes of HCC, ^{68}Ga-PSMA-11 PET is a new diagnostic modality; however, correlation with tumor differentiation and aggressiveness requires further assessment.

Our study was limited by its retrospective design and the small number of patients included. Histopathology was available for only a small group of patients, as tissue sampling is not routinely performed and biopsy of extrahepatic lesions is difficult because of their small size or remote location. Thus, most lesion follow-up was based on correlative or follow-up imaging with known intrinsic limitations. In addition, MRI or PET/MRI was not systematically performed for comparison in the included patients. Finally, 18 of 40 (45%) patients had an uptake time outside the range of 50 to 100 min recommended by the European Association of Nuclear Medicine and the Society of Nuclear Medicine and Molecular Imaging (*14*), which may have impacted image interpretation.

CONCLUSION

Using masked reads and independent lesion validation, we established the accuracy of ^{68}Ga-PSMA-11 PET for HCC staging, which was comparable to the accuracy of CT for hepatic disease detection and more accurate for extrahepatic disease detection. ^{68}Ga-PSMA-11 PET induced stage migration by detection of distant metastases in 11 of 40 patients (27.5%), and this migration was associated with a shift from local to systemic therapy in 8 of 11 (73%) of these patients. ^{68}Ga-PSMA-11 PET may prove valuable for early identification of candidates for systemic therapy.

DISCLOSURE

Ken Herrmann reports personal fees from Bayer, SIRTEX, Adacap, Curium, Endocyte, IPSEN, Siemens Healthineers, GE Healthcare, Amgen, Novartis, and ymabs, as well as personal and other fees from Sofie Biosciences, nonfinancial support from ABX, and grants and personal fees from BTG, all of which are outside the submitted work. Christian M. Lange has received speaker and consultancy fees from Abbvie, MSD, Roche, Eisai, Behring, Falk, Novartis, and Norgine, all of which are outside the submitted work. Manuel Weber is on the Speakers Bureau for Boston Scientific. Wolfgang P. Fendler is a consultant for Endocyte and BTG, and he received personal fees from RadioMedix, Bayer, and Parexel, as well as financial support from Mercator Research Center Ruhr (MERCUR, An-2019-0001), IFORES (D/107-81260, D/107-30240), Doktor Robert Pfleger-Stiftung, and Wiedenfeld-Stiftung/Stiftung Krebsforschung Duisburg, all of which are outside the submitted work. No other potential conflict of interest relevant to this article was reported.

KEY POINTS

QUESTION: Does ^{68}Ga-PSMA-11 PET/CT improve tumor detection and impact the clinical management of patients with HCC?

PERTINENT FINDINGS: The staging accuracy of ^{68}Ga-PSMA-11 PET was comparable to that of CT for hepatic staging and more accurate for extrahepatic staging, inducing stage migration by detection of distant metastases in 11 of 40 patients (27.5%), with a shift from local to systemic therapy in 8 of 11 (73%) of these patients. ^{68}Ga-PSMA-11 PET may prove valuable for early identification of candidates for systemic therapy.

IMPLICATIONS FOR PATIENT CARE: ^{68}Ga-PSMA-11 PET demonstrated higher accuracy than CT in the detection of HCC metastases and was associated with a management change in about half the patient cohort.

REFERENCES

1. Forner A, Llovet JM, Bruix J. Hepatocellular carcinoma. *Lancet.* 2012;379:1245–1255.
2. Bruix J, Sherman M. Management of hepatocellular carcinoma: an update. *Hepatology.* 2011;53:1020–1022.
3. Lencioni R, Chen XP, Dagher L, Venook AP. Treatment of intermediate/advanced hepatocellular carcinoma in the clinic: how can outcomes be improved? *Oncologist.* 2010;15(suppl 4):42–52.
4. Vogel A, Cervantes A, Chau I, et al. Hepatocellular carcinoma: ESMO clinical practice guidelines for diagnosis, treatment and follow-up. *Ann Oncol.* 2018;29:iv238–iv255.
5. Perera M, Papa N, Roberts M, et al. Gallium-68 prostate-specific membrane antigen positron emission tomography in advanced prostate cancer: updated diagnostic utility, sensitivity, specificity, and distribution of prostate-specific membrane antigen-avid lesions—a systematic review and meta-analysis. *Eur Urol.* 2020;77:403–417.
6. Perera M, Papa N, Christidis D, et al. Sensitivity, specificity, and predictors of positive ^{68}Ga-prostate-specific membrane antigen positron emission tomography in advanced prostate cancer: a systematic review and meta-analysis. *Eur Urol.* 2016;70:926–937.
7. Chang SS, O'Keefe DS, Bacich DJ, Reuter VE, Heston WDW, Gaudin PB. Prostate-specific membrane antigen is produced in tumor-associated neovasculature. *Clin Cancer Res.* 1999;5:2674–2681.
8. Chang SS, Reuter VE, Heston WD, Bander NH, Grauer LS, Gaudin PB. Five different anti-prostate-specific membrane antigen (PSMA) antibodies confirm PSMA expression in tumor-associated neovasculature. *Cancer Res.* 1999;59:3192–3198.
9. Kesler M, Levine C, Hershkovitz D, et al. ^{68}Ga-PSMA is a novel PET-CT tracer for imaging of hepatocellular carcinoma: a prospective pilot study. *J Nucl Med.* 2019;60:185–191.
10. Tolkach Y, Goltz D, Kremer A, et al. Prostate-specific membrane antigen expression in hepatocellular carcinoma: potential use for prognosis and diagnostic imaging. *Oncotarget.* 2019;10:4149–4160.
11. Kunikowska J, Cieslak B, Gierej B, et al. [^{68}Ga]Ga-prostate-specific membrane antigen PET/CT: a novel method for imaging patients with hepatocellular carcinoma. *Eur J Nucl Med Mol Imaging.* 2021;48:883–892.
12. Harris PA, Taylor R, Minor BL, et al The REDCap consortium: building an international community of software platform partners. *J Biomed Inform.* 2019;95:103208.
13. Harris PA, Taylor R, Thielke R, Payne J, Gonzalez N, Conde JG. Research electronic data capture (REDCap): a metadata-driven methodology and workflow process for providing translational research informatics support. *J Biomed Inform.* 2009;42:377–381.
14. Fendler WP, Eiber M, Beheshti M, et al. ^{68}Ga-PSMA PET/CT: joint EANM and SNMMI procedure guideline for prostate cancer imaging: version 1.0. *Eur J Nucl Med Mol Imaging.* 2017;44:1014–1024.

15. Eiber M, Herrmann K, Calais J, et al. Prostate cancer molecular imaging standardized evaluation (PROMISE): proposed miTNM classification for the interpretation of PSMA-ligand PET/CT. *J Nucl Med.* 2018;59:469–478.
16. Fendler WP, Calais J, Eiber M, et al. Assessment of ^{68}Ga-PSMA-11 PET accuracy in localizing recurrent prostate cancer: a prospective single-arm clinical trial. *JAMA Oncol.* 2019;5:856–863.
17. Willatt J, Ruma JA, Azar SF, Dasika NL, Syed F. Imaging of hepatocellular carcinoma and image guided therapies: how we do it. *Cancer Imaging.* 2017;17:9.
18. Choi JY, Lee JM, Sirlin CB. CT and MR imaging diagnosis and staging of hepatocellular carcinoma: part I. Development, growth, and spread: key pathologic and imaging aspects. *Radiology.* 2014;272:635–654.
19. Amin MB, Edge S, Greene F, et al. *AJCC Cancer Staging Manual.* 8th ed. Springer International Publishing; 2017:287–294.
20. Lencioni R, Llovet JM. Modified RECIST (mRECIST) assessment for hepatocellular carcinoma. *Semin Liver Dis.* 2010;30:52–60.
21. Landis JR, Koch GG. The measurement of observer agreement for categorical data. *Biometrics.* 1977;33:159–174.
22. Clark T, Maximin S, Meier J, Pokharel S, Bhargava P. Hepatocellular carcinoma: review of epidemiology, screening, imaging diagnosis, response assessment, and treatment. *Curr Probl Diagn Radiol.* 2015;44:479–486.
23. European Association for the Study of the Liver. EASL clinical practice guidelines: management of hepatocellular carcinoma. *J Hepatol.* 2018;69:182–236.
24. Heimbach JK, Kulik LM, Finn RS, et al. AASLD guidelines for the treatment of hepatocellular carcinoma. *Hepatology.* 2018;67:358–380.
25. Verslype C, Rosmorduc O, Rougier P, Group EGW. Hepatocellular carcinoma: ESMO-ESDO clinical practice guidelines for diagnosis, treatment and follow-up. *Ann Oncol.* 2012;23(suppl 7):vii41–vii48.
26. Boland P, Wu J. Systemic therapy for hepatocellular carcinoma: beyond sorafenib. *Chin Clin Oncol.* 2018;7:50.
27. Ingle PV, Samsudin SZ, Chan PQ, et al. Development and novel therapeutics in hepatocellular carcinoma: a review. *Ther Clin Risk Manag.* 2016;12:445–455.
28. Llovet JM, Ricci S, Mazzaferro V, et al. Sorafenib in advanced hepatocellular carcinoma. *N Engl J Med.* 2008;359:378–390.
29. Kudo M, Finn RS, Qin S, et al. Lenvatinib versus sorafenib in first-line treatment of patients with unresectable hepatocellular carcinoma: a randomised phase 3 non-inferiority trial. *Lancet.* 2018;391:1163–1173.
30. Cheng A-L, Kang Y-K, Chen Z, et al. Efficacy and safety of sorafenib in patients in the Asia-Pacific region with advanced hepatocellular carcinoma: a phase III randomised, double-blind, placebo-controlled trial. *Lancet Oncol.* 2009;10:25–34.
31. Li D, Sedano S, Allen R, Gong J, Cho M, Sharma S. Current treatment landscape for advanced hepatocellular carcinoma: patient outcomes and the impact on quality of life. *Cancers (Basel).* 2019;11:841.
32. Mahalingam D, Peguero J, Cen P, et al. A phase II, multicenter, single-arm study of mipsagargin (G-202) as a second-line therapy following sorafenib for adult patients with progressive advanced hepatocellular carcinoma. *Cancers (Basel).* 2019;11:833.
33. Roberts LR, Sirlin CB, Zaiem F, et al. Imaging for the diagnosis of hepatocellular carcinoma: a systematic review and meta-analysis. *Hepatology.* 2018;67:401–421.
34. Filippi L, Schillaci O, Bagni O. Recent advances in PET probes for hepatocellular carcinoma characterization. *Expert Rev Med Devices.* 2019;16:341–350.
35. Chalaye J, Costentin CE, Luciani A, et al. Positron emission tomography/computed tomography with ^{18}F-fluorocholine improve tumor staging and treatment allocation in patients with hepatocellular carcinoma. *J Hepatol.* 2018;69:336–344.